Colloids and Surfaces B: Biointerfaces 73 (2009) 376–381

Contents lists available at ScienceDirect

Colloids and Surfaces B: Biointerfaces

journal homepage: www.elsevier.com/locate/colsurfb

Controlled release of dual drugs from emulsion electrospun nanofibrous mats

Su Yan[a,b,c], Li Xiaoqiang[a,b,c], Liu Shuiping[a,b], Mo Xiumei[a,b,c,*], Seeram Ramakrishna[c,d]

[a] State Key Laboratory for Modification of Chemical Fibers and Polymer Materials, Donghua University, Shanghai 201620, China
[b] College of Material Science and Engineering, Donghua University, Shanghai 201620, China
[c] Biomaterials and Tissue Engineering Laboratory, College of Chemistry, Chemical Engineering and Biotechnology, Donghua University, Shanghai 201620, China
[d] Nanoscience and Nanotechnology Initiative, National University of Singapore, Singapore 117576, Singapore

ARTICLE INFO

Article history:
Received 15 March 2009
Received in revised form 4 June 2009
Accepted 5 June 2009
Available online 13 June 2009

Keywords:
Control release
Emulsion electrospinning
Nanofibers
PLLACL

ABSTRACT

The purpose of this work is to develop a novel type of tissue engineering scaffold or drugs delivery carrier with the capability of encapsulation and controlled release drugs. In this study, Rhodamine B and Bovine Serum Albumin (BSA) were successfully incorporated into nanofibers by means of emulsion electrospinning. The morphology of composite nanofibers was studied by Scanning Electron Microscopy (SEM). The composite nanofibrous mats made from emulsion electrospinning were characterized by water contact angle measurement and X-ray diffraction. In vitro dual drugs release behaviors from composite nanofibrous mats were investigated. The results indicated that the incorporated drug and/or proteins in composite fibrous mats made from electrospinning could be control released by adjusting the processes of emulsions preparation.

1. Introduction

Electrospinning is a method which combined two techniques namely electrospray and sinning [1]. The conventional spinning processes including wet-, dry- and wet/dry-spinning techniques are capable of producing fibers with diameter in the micrometer rang. Unlike the conventional spinning, electrospinning is capable of producing fibers with the diameter ranged from tens nanometer to several micrometer [2–4]. Additionally, the non-woven fibrous mats made of electrospun polymer nanofibers offer a unique capability to control the fibers diameters by adjusting applied voltages, collecting distances, solutions concentrations and solutions flow rates [5]. Unlike nanorods, nanotubes, and nanowires that are produced mostly by synthetic, bottom-up methods, electrospun nanofibers are produced through a top-down nano-manufacturing process, which results in continuous and low-cost nanofibers that are also relatively easy to align, assemble and process into applications [6–8].

Drug delivery systems have numerous advantages compared with conventional dosage forms, such as improve therapeutic effect, reduce toxicity and improve patient compliance, by delivering drugs at a controlled rate over a period of time to the site of action [6,9–11]. With respect to the local delivery of bioactive ingredient (such as growth factors), electrospun ultrafine fibers have been investigated as tissue engineering scaffolds and biofunctional scaffolds for other biomedical applications [12–14]. Plenty of polymeric materials, either non-degradable or biodegradable materials, can be used as delivery matrices. In the delivery system made from non-degradable materials, for example, drugs mainly released and driven by a concentration gradient. However, drugs release from biodegradable matrices by both diffusion and scaffolds degradation. For polymeric materials used in tissue engineering applications, biodegradable materials are generally more popular due to the reason that they eliminate gradually for the need of new tissue regeneration and replace the scaffolds.

For drug delivery devices, there is a particular interest in producing core-shell type nanofibers which could encapsulate in the core part of fibers, and sustained release drugs and/or bio-growth factors for a long time [15]. Furthermore, core-shell structures devices are generally more adaptive for incorporating proteins. They could preserve an unstable biological agent from aggressive environments, and functionalize the surface of nanostructures without affecting the core material. Coaxial electrospinning had been reported for preparing core-shell structures nanofibers, in which two components can be coaxially and simultaneously electrospun through different feeding capillary channels [16]. The coaxial electrospinning was a dynamic process, and many factors such as flow rate of the inner and outer solutions, interfacial tension, and viscoelasticity of the two polymer solutions could affect entrainment and produce fibers without the required core-shell structure [17,18]. In addition, a special apparatus and careful selection of operational parameters were also needed to ensure the desired results. Recently, preparing core-shell type nanofibers by emulsion electrospinning has

* Corresponding author at: College of Chemistry, Chemical Engineering and Biotechnology, Donghua University, Shanghai 201620, China. Tel.: +86 21 67792653.
E-mail address: xmm@dhu.edu.cn (M. Xiumei).

0927-7765/$ – see front matter © 2009 Elsevier B.V. All rights reserved.
doi:10.1016/j.colsurfb.2009.06.009

attracted growing interests [19–21]. The emulsions (especially the water-in-oil type of emulsions) usually contain an oil phase which is obtained by dissolving polymers (particularly biocompatible and biodegradable) into organic solvent, and a water phase (or the emulsion spheres) with sizes of microns or sub-microns which have drug or protein dissolved. Under the electric force during the process of electrospinning, emulsion with the oil phase of polymer solution and the water phase of micron or sub-micron spheres could be elongated. These nanofibers with drugs and proteins encapsulated would be fabricated into bioactive tissue engineering scaffolds. It is remarkable that unlike coaxial electrospinning which need a special apparatus, the basic equipment for emulsion electrospinning only need a single needle [22].

However, the previous studies mostly focus on encapsulating and releasing only one drug or protein by the means of electrospinning. In the present study, two agent including Bovine Serum Albumin (BSA) and Rhodamine B were incorporated into PLLACL nanofibers with the method of emulsion electrospinning. Sorbitan monooleate (Span-80, a non-ionic emulsifier/surfactant that had been demonstrated non-toxic and safe for cell-growth in our previous report [23]), poly(l-lactide-co-caprolactone) [PLLACL], methylene dichloride and distilled water were used to prepare electrospinning emulsions. The morphologies of the as-spun nanofibrous mats were examined by scanning electron microscopy (SEM). Fibers diameters and their distribution were determined by measuring fibers on the SEM images. The surface hydrophilicity was measured by the water contact angle method. The nanofibers were also been characterized by X-ray diffraction. The BSA and Rhodamine B encapsulation/release profiles from the electrospun nanofibrous mats immersed in phosphate buffered saline (pH 7.4) for various time periods were recorded and analyzed.

2. Experimental

2.1. Materials

PLLACL with molar ratio of 75% being L-lactide was purchased from the Sigma–Aldrich Co. (Milwaukee, Wisconsin). Span-80 was purchased from the Zibo Haijie Chemical Industry Co., Ltd. (Zibo, China). Methylene dichloride was purchased from the Shanghai Fine-Chemicals Co., Ltd. (Shanghai, China). Rhodamine B and BSA was purchased from Sigma–Aldrich. All of the materials and solvent were used without further purification.

2.2. Preparation of electrospinning solutions/emulsions

E emulsion was prepared by dissolving 0.8 g PLLACL into 10 mL methylene dichloride, thereafter, 0.008 g Rhodamine B and 0.04 mL Span80 was added into the previous solution to make the oil solution. BSA was dissolved in distilled water to become 5 wt% aqueous solution. Subsequently, 0.5 mL aqueous solution added into polymer solution (or the oil solution) dropwise. The mixture was stirred at 240 rpm for 2 h to obtain uniform emulsions.

D emulsion was prepared by dissolving BSA and Rhodamine B into distilled water together to make a solution consisted of 5 wt% BSA and 1 wt% Rhodamine B as the aqueous phase. PLLACL and 0.04 mL Span80 were dissolved in methylene dichloride to prepare 8 wt% solution as the oil phase. 0.5 mL aqueous solution added dropwise into polymer solution. The mixture was stirred at 240 rpm for 2 h to obtain uniform emulsions.

Two control samples (B and C) were prepared as the following: Under the same operation conditions, 0.5 mL 5% BSA aqueous solutions and 1% Rhodamine B respect to the polymer carrier were emulsified into 10 mL of 8 wt% methylene dichloride solution of PLLACL, respectively, forming the W/O emulsions. PLLACL was dissolved in methylene dichloride to form A solution with the concentration of 8 wt%. Although Rhodamine B is soluble in both water and ethylene dichloride, we believe that the majority of it was in the aqueous phase in the solution of C and D, and the majority of it was in the oil phase in the solution of E, because of the procedures for preparing the emulsions.

The details of the solutions A, B, C, D and E were shown in Table 1.

Table 1
Component of solution and emulsions for electrospinning.

Solutions	Oil phase	Water phase
A	PLLACL	–
B	PLLACL	BSA
C	PLLACL	Rhodamine B
D	PLLACL	BSA and Rhodamine B
E	PLLACL and Rhodamine B	BSA

2.3. Electrospinning of nanofibrous mats

The experimental set-up used for conducting electrospinning included a high voltage power supply (BGG DC high-voltage generator), purchased from the BMEI Co., Ltd. (Beijing, China), and a digitally controlled and extremely accurate syringe pump KDS 200), purchased from KD Scientific (Holliston, MA). During electrospinning, a positive high voltage of 20 kV was applied at the tip of a syringe needle with the inner diameter of 0.9 mm. The electrospun nanofibers were collected on a piece of aluminum foil covered on an electrically grounded metal plate, which was placed at a distance of 15 cm below the tip of the syringe needle. The mass flow rate was maintained at 1.0 mL/h. The electrospinning was conducted under the ambient conditions.

2.4. Morphologies of as-spun nanofibrous mats

A JSM-5600 LV digital vacuum Scanning Electron Microscope (SEM), produced by the Japan Electron Optical Laboratory (JEOL), was employed to examine the morphologies of the prepared nanofibers mats. Prior to SEM examination, the specimens were sputter-coated with gold to avoid charge accumulation. The diameter of the electrospun ultrafine nanofibers was measured with image visualization software Image-J 1.34 (National Institutes of Health, USA). Average fiber diameter and diameter distribution were determined by measuring about 100 random fibers from the SEM images.

2.5. Characterization of composite fibers

Water contact angles of nanofibrous mats were measured using a contact angle analyzer made by the Data Physics Corp. (San Jose, CA) to identify the effect of Span80 addition on the hydrophilicity of electrospun nanofibrous mats. During the measurements, the samples of nanofibrous mats were first cut into square pieces with the size of 1 cm^2, followed by placing them on a testing plate. Subsequently, 0.03 mL distilled water was carefully dropped onto the prepared specimens. The contact angles between water droplets and nanofibrous mats were measured and recorded by a video monitor.

The samples were tested using an X-ray diffraction instrument (D/MAX-2550PC, Rigaku, Japan) under the condition of Cu Kα1, 40 kV and 300 mA. In this work, PLLACL fibers and composite fibers with protein/drug incorporated were studied. The samples were scanned from 5° to 60 ° at a scanning rate of 5°/min.

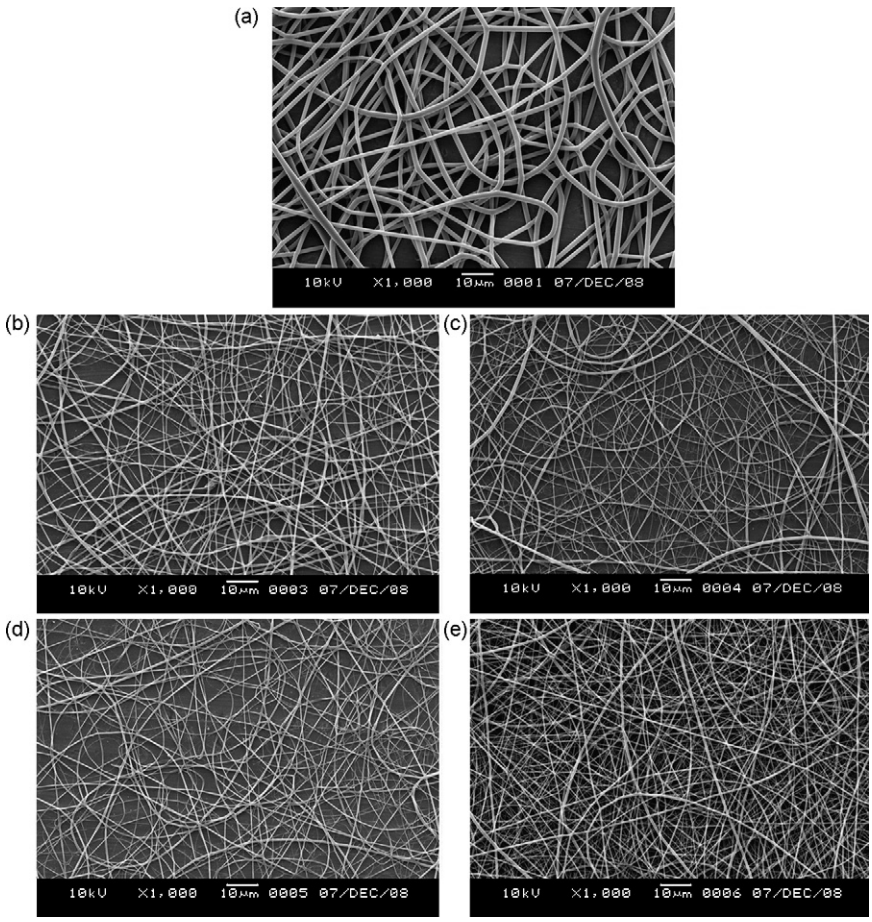

Fig. 1. Representative morphologies of the nanofibrous mats electrospun from the solutions of A, B, C, D and E.

2.6. Release behavior study

For the drugs release behavior study, composite nanofibrous mat electrospun from the solutions D and E as well as the two control samples (B and C), each weighing about 100 mg, were soaked in glass vials with 100 mL of PBS. The fibrous mats were incubated at 37 °C in the presence of 5% carbon dioxide. At various time points, 2 mL of supernatant was retrieved from the vial followed by diluting them to 10 mL using PBS, and an equal volume of fresh medium was replaced. The concentration of Rhodamine B (at an optical wavelength of 550 nm) and BSA (at an optical wavelength of 280 nm) in the supernatant were then determined by an UV–vis spectrophotometer (WFZ UV-2102 Unique Technology Shanghai) respectively.

2.7. Morphologies of nanofibrous mats after releasing

Morphology of nanofibrous mats after drug and/or protein releasing in PBS for 14 days was observed by Digital Vacuum Scanning Electron Microscope (JSM-5600LV, Japan Electron Optical Laboratory) at the accelerating voltage of 15 kV. Prior to SEM examination, the specimens were sputter-coated with gold to avoid charge accumulation.

3. Result and discussion

3.1. Morphology study of electrospun fibers

During the process of electrospinning, particularly during "bending instability" [24], the spherically shaped emulsion particles (or droplets) would be significantly elongated, and parts of them would be broken into smaller particles and/or droplets under the electric forces. These small particles and/or droplets would eventually result in the formation of the composite nanofibers with proteins and/or drugs incorporated. It is noted that the emulsion jets would rapidly solidify accompanied with the evaporation of solvents which including distilled water and methylene dichloride in the present study. The solidified emulsion jets would became ultrafine fibers made up of PLLACL, Span80, BSA and Rhodamine B (or part of them). Fig. 1 shows the SEM images of the nanofibrous mats electrospun from the solutions of A, B, C, D and E.

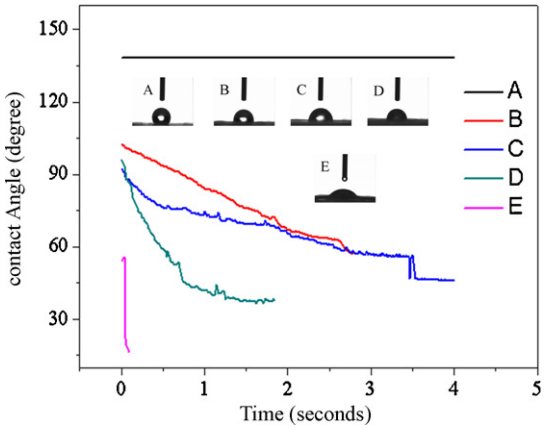

Fig. 2. Water contact angles of the nanofibrous mats electrospun from A, B, C, D and E, the inset shows the optical observations of the water contact angles immediately after the water droplets were placed on the nanofibrous mats.

From images of (b–e), the nanofibers looked uniform, and their surfaces were smooth. Their smooth and uniform surfaces indicated that BSA and or Rhodamine B were successfully incorporated into results fibers. Moreover, it seemed that the fibers electrospun from different solutions did not show appreciable difference in morphology and average diameter except "a". The average diameter of fibers electrospun from A solution was much larger than others, because Span80 molecule has a highly hydrophilic end that can strongly interact with the molecule of Rhodamine B and BSA, Span-80/Rhodamine B and/or BSA complexes would carry excess charges during the process of electrospinning [25]. And it is well known that higher conductivity could elongate polymer jet easier and generate much thinner nanofibers.

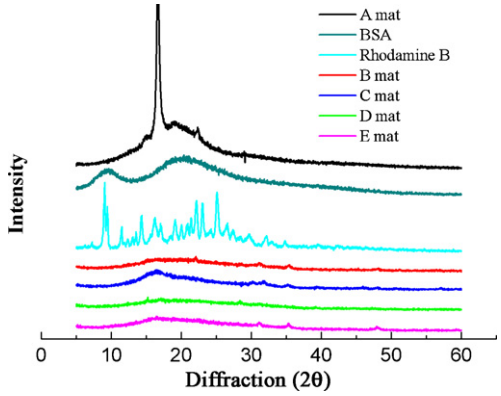

Fig. 3. XRD patterns of BSA, Rhodamine B, and the nanofibrous mats electrospun from solutions or emulsions described in Section 2.2.

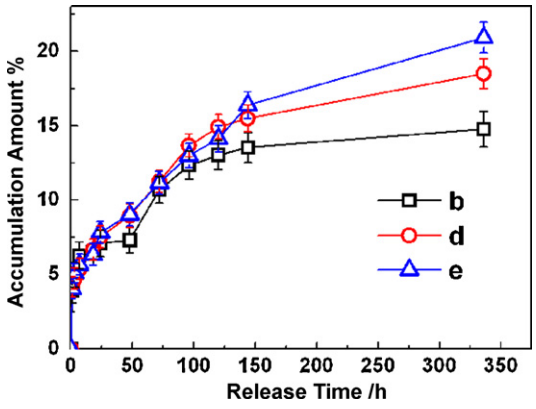

Fig. 4. Cumulative BSA release profiles from composite fibrous mats. BSA was released from the nanofibrous mats generated by solution/emulsion of B, D and E which described in Section 2.2.

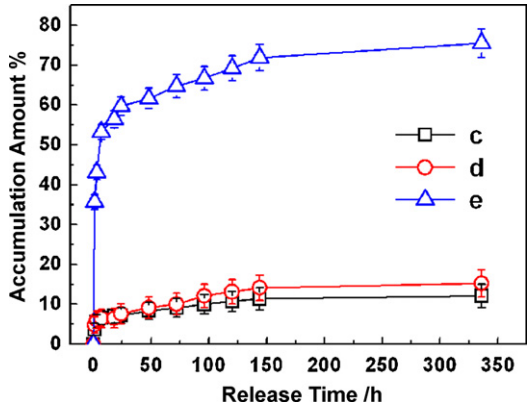

Fig. 5. Cumulative Rhodamine B release profiles from composite fibrous mats. Rhodamine B was released from C, D and E.

3.2. Characterization of composite fibers

The hydrophilicity of nanofibrous mats plays a pivotal role to determine their overall performances as tissue engineering scaffolds. The water-contact-angle technique had been used for testing the hydrophilicity of nanofibrous mats [26-28]. The detailed procedures have been described in the Experimental section. The inset in Fig. 2 showed the visual observations of the water contact angle variations after the water droplets were placed on the nanofibrous mats at the very beginning of hydrophilicity tests. It was evident that the PLLACL nanofibrous mats incorporated drugs

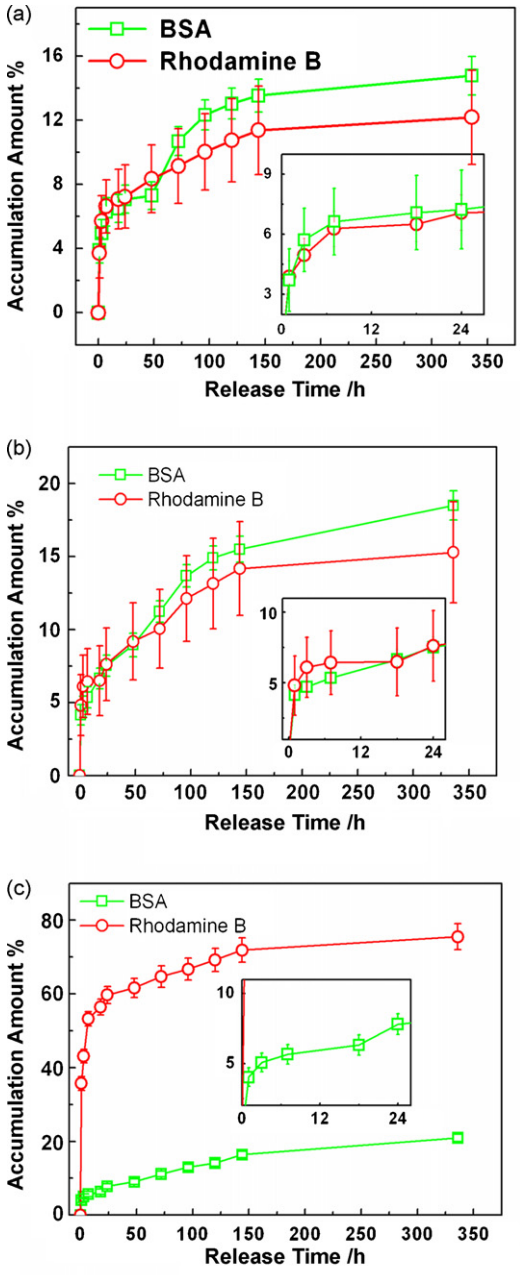

Fig. 6. Release profiles of BSA and Rhodamine B from composite nanofibrous mats. (a) Release profiles of BSA from B mat and Rhodamine B from C mats; (b) release profiles of BSA and Rhodamine B from D mat; (c) release profiles of BSA and Rhodamine B from E mat.

were much more hydrophilic than the neat PLLACL nanofibrous mats. As shown in Fig. 2, after the water droplets were placed on the nanofibrous mats, the water contact angle of samples B–E (nanofibrous mats incorporated drugs) reduced sharply, especially on sample E. However, the water contact angle on nanofibrous mat (sample A) shows no significant change for more than 4 s.

XRD patterns of the electrospun composite nanofibrous mats (B, C, D and E mat); powders of BSA and Rhodamine B; and PLLACL nanofibrous mat (A mat) were displayed in Fig. 3. Electrospun PLLACL nanofibers (A) was crystalline, showing an intensity peak at 2θ of 16.6° and a lower intensity at 2θ of 22.3°. It was shown that Rhodamine B was crystalline, with many characteristic peaks, while BSA was amorphous. The crystalline Rhodamine B was not detected in all Rhodamine B-loading PLLACL fibers (C, D and E), because there was only 0.1–1.0% Rhodamine B in the results nanofibrous mats. BSA was amorphous, without characteristic peak, and BSA loaded fibers (B) were also showed amorphous form. Drugs existed in amorphous state in the composite nanofibers, and there was not any chemical reaction or intermolecular action between polymer and drugs.

3.3. In vitro release study

Release behaviors of BSA and Rhodamine B from composite fibrous mats were studied and shown in Figs. 4–6. Fig. 4 shows cumulative release profiles of BSA from electrospun composite fibrous mats (B, D and E). The release profiles of BSA from these nanofibrous mats show no significant difference in the first 96 h. It is noted that BSA was loaded in the aqueous phase in all of three nanofibrous mats. Therefore, we believed that the encapsulations of Rhodamine B have no impact the release behavior of BSA, when BSA and Rhodamine B were incorporated in the same nanofibrous mats with the method of emulsion electrospinning. However, after the first 96 h releasing, there was more BSA released from dual drugs loading nanofibrous mats (D and E) than those released from single drug loading nanofibrous mat B. E released about 20% of loaded BSA at 336 h and D released about 18%, while B released about 14%. The results indicated that the incorporated BSA was released by molecular diffusion through the matrix, and there was a slight impact caused by other drug (in this study, Rhodamine B) which was loaded in the same nanofibrous composite.

Fig. 5 shows the cumulative release profiles of Rhodamine B from electrospun composite fibrous mats (C, D and E). The release profiles of Rhodamine B from C and D mats were similar, and both of them present the sustained release behavior with the ultimate release percentage about 12% after immersing in PBS for 336 h. As aforementioned in Section 2.2, the emulsions of C and D were prepared by dissolving Rhodamine B in the aqueous solutions; therefore, we believed that Rhodamine B was located in the core part of the nanofibers, and Rhodamine B was release mostly by diffusion from the nanofibrous matrix. It can be expected that the Rhodamine B would release as the degradation of PLLACL nanofibers in the later period. However, there was an obvious burst release in the very beginning of profile of E, because the Rhodamine B was inclined to move to and locate on the surface of nanofibers under the driving of electric force in the process of electrospinning. And it is easy to understand that the drugs which located on the surface of nanofibers dissolved into puffer solution directly.

Fig. 6(a) shows cumulative release profile of BSA and Rhodamine B from B and C. it was detected that BSA were releasing as same manner from the nanofibrous mats without showing initial burst for a long time. There was 14% of BSA and 12% of Rhodamine B released from the nanofibers at the end of our study, respectively. It was obvious that the release processes were not complete, and rest of them would release with the degradation of polymer fibers. Fig. 6(b) gives the drug release profiles of BSA and Rhodamine B from nanofibrous mat D. It is seen that they present a similar release behavior. Only 18% of BSA and 15% Rhodamine B was released, respectively. Fig. 6(c) shows the total release profile of dual drugs from nanofibrous mat "E". In Fig. 6(c), the release profile of BSA from nanofibers matrix present a sustained release manner, while Rhodamine B had a burst release at the beginning. At the end of the release study, the ultimate release percentage of Rhodamine B was about 80%, and the percentage of BSA was only 20%. This result of BSA release behavior in Fig. 6(c) was consistent with Fig. 6(a and b), because BSA was incorporated in the core parts of all of the three nanofibrous samples (B, D and E). The results demonstrated that the release behaviors of drug and/or protein were influenced and varied by their incorporated types. When the drug and/or protein were encapsulated in the core of nanofibers, the release profile would present a sustained manner; however, when drug and/or proteins

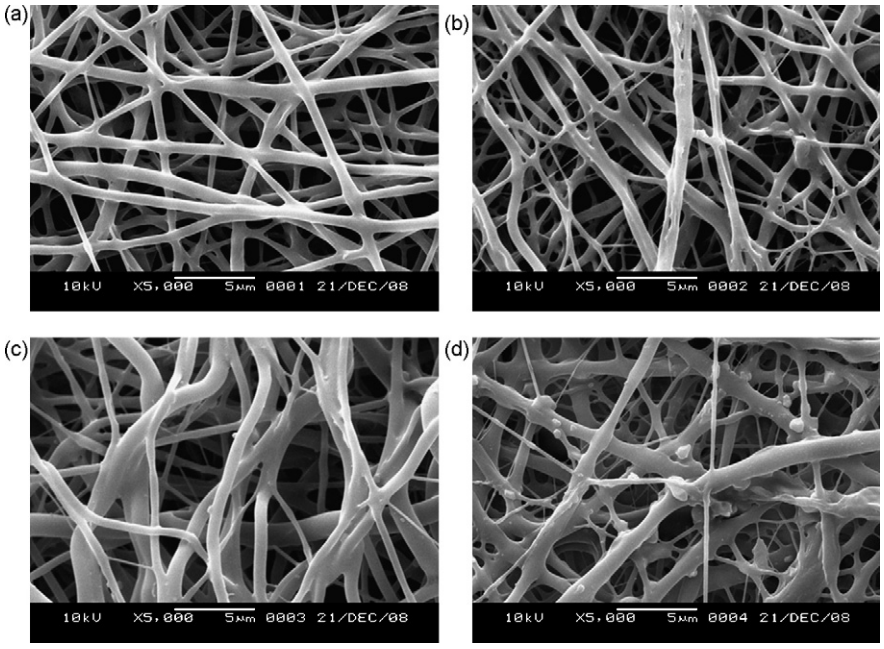

Fig. 7. SEM images showing representative morphologies of the nanofibrous mats electrospun from B, C, D, and E after drugs release in PBS (pH 7.4).

Table 2
Average diameters of composite nanofibers before and after immersion in PBS (PH 7.4) over 14days.

	B mat (nm)	C mat (nm)	D mat (nm)	E mat (nm)
Before immersion	670	452	512	481
After immersion	862	762	920	943

located in the surface of nanofibers, there would be a burst release in the beginning.

3.4. Morphologies of nanofibrous mats after releasing

In this study, the degradability and morphological sustainability of the electrospun composite nanofibrous mats were also investigated after immersion in PBS for 14 days. Degradation profiles of the composite nanofibrous mats were evaluated macroscopically by SEM and shown in Fig. 7. In contrast to the smooth surface of fibers before incubation as shown in Fig. 1, visible changes of the morphologies of nanofibrous mats were observed. As shown in Fig. 7(a), the electrospun composite nanofibrous mat B (image a) almost retained the original morphology after incubation in PBS of pH 7.4 for 336 h. However, the average diameter of nanofibers after immersing in PBS was larger than before immersion (the details were shown in Table 2). Nanofibrous mats C, D and E (images b, c and d) obviously lost their original morphologies after immersing in PBS (shown in Fig. 7(b–d)). It is obviously to detect the nanofibers in Fig. 7(b–d) were degraded much more serious than those in Fig. 7(a). In Liao et al. report [25], they supposed that surfactant molecules covered on the nanofibers surface could prevent the penetration/diffusion of water molecules, thus could prevent the degradation of polymer nanofibers. In the present study, it was found that the hydrophilicity also impact the degradation of nanofibrous mats. As shown in Fig. 2, mats C, D and E were much more hydrophilic than mat B. The results of hydrophilicity test and degradation observations demonstrated that the high hydrophilicity promoted the degradation of nanofibrous mats.

4. Conclusion

In this study, a composite nanofibrous mat was prepared by electrospinning an emulsion made of PLLACL, Rhodamine B, Span-80, BSA, methylene dichloride and distilled water. Its morphology was examined by SEM, its surface hydrophilicity was measured by the water contact angle method, and its protein and/or drug encapsulation/release profile in PBS (pH 7.4) was recorded and analyzed. The results indicated that the composite nanofibers electrospun from the emulsion had diameters of 481 nm, and they were smooth and uniform without microscopically identifiable beads and/or beaded-nanofibers). The release behaviors of five types of electrospun nanofibrous mats revealed that the composite nanofibrous mats electrospun from the emulsion exhibited the most desired and controllable release performance. Furthermore, the different incorporated methods (in the aqueous phase or the oil phase) led to different release behaviors of the result nanofibrous mats. Due to these results, the composite nanofibrous mat is expected to carry dual hydrophilic and hydrophobic drugs and proteins. It is promising to be used in the biomedical applications or pharmaceutical devices, such as tissue engineering scaffold and drug delivery vehicle.

Acknowledgements

This research was supported by National Science Foundation (30570503), National High Technology Research and Developed Program (863 Program, 2008AA03Z305), Science and Technology Commission of Shanghai Municipality Program (08520704600, and 0852nm03400).

References

[1] D.H. Reneker, A.L. Yarin, E. Zussman, H. Xu, Advances in Applied Mechanics 41 (2007) 43.
[2] T.J. Sill, H.A. von Recum, Biomaterials 29 (2008) 1989.
[3] Z.M. Huang, Y.Z. Zhang, S. Ramakrishna, Journal of Polymer Science Part B: Polymer Physics 43 (2005) 2852.
[4] Z.M. Huang, Y.Z. Zhang, S. Ramakrishna, C.T. Lim, Polymer 45 (2004) 5361.
[5] X.M. Mo, C.Y. Xu, M. Kotaki, S. Ramakrishna, Biomaterials 25 (2004) 1883.
[6] S. Shamnugasundaram, K.A. Griswold, C.J. Prestigiacomo, T. Arinzeh, M. Jaffe, Proceedings of the IEEE 30th Annual Northeast Bioengineering Conference, 2004, p. 140.
[7] N. Ashammakhi, A. Ndreu, L. Nikkola, I. Wimpenny, Y. Yang, Regenerative Medicine 3 (2008) 547.
[8] A.S. Badami, M.R. Kreke, M.S. Thompson, J.S. Riffle, A.S. Goldstein, Biomaterials 27 (2006) 596.
[9] C.L. He, Z.M. Huang, L. Liu, X.J. Han, Proceedings of 2005 International Conference on Advanced Fibers and Polymer Materials (ICAFPM 2005), vols. 1 and 2, 2005, pp. 708–712.
[10] X. Xu, X. Chen, P. Ma, X. Wang, X. Jing, European Journal of Pharmaceutics and Biopharmaceutics 70 (2008) 165.
[11] A. Martins, J.V. Araujo, R.L. Reis, N.M. Neves, Nanomedicine 2 (2007) 929.
[12] D. Liang, B.S. Hsiao, B. Chu, Advanced Drug Delivery Reviews 59 (2007) 1392.
[13] H.W. Kim, H.H. Lee, J.C. Knowles, Journal of Biomedical Materials Research: Part A 79 (2006) 643.
[14] E. Luong-Van, L. Grondahl, K.N. Chua, K.W. Leong, V. Nurcombe, S.M. Cool, Biomaterials 27 (2006) 2042.
[15] Z.M. Huang, A.H. Yang, Acta Polymer Sinica 1 (2006) 48.
[16] Z.M. Huang, C.L. He, A.Z. Yang, Y.Z. Zhang, X.J. Hang, J.L. Yin, Q.S. Wu, Journal of Biomedical Materials Research: Part A 77A (2006) 169.
[17] C.L. He, Z.M. Huang, X.J. Han, L. Liu, H.S. Zhang, L.S. Chen, Journal of Macromolecular Science Part B: Physics 45 (2006) 515.
[18] H.L. Jiang, Y.Q. Hu, P.C. Zhao, Y. Li, K.J. Zhu, Journal of Biomedical Materials Research Part B: Applied Biomaterials 79B (2006) 50.
[19] X.L. Xu, L.X. Yang, X.Y. Xu, X. Wang, X.S. Chen, Q.Z. Liang, J. Zeng, X.B. Jing, Journal of Controlled Release 108 (2005) 33.
[20] H. Qi, P. Hu, J. Xu, A. Wang, Biomacromolecules 7 (2006) 2327.
[21] X.L. Xu, X.L. Zhuang, X.S. Chen, X.R. Wang, L.X. Yang, X.B. Jing, Macromolecular. Rapid Communication 27 (2006) 1637.
[22] Y. Yang, X. Li, W. Cui, S. Zhou, R. Tan, C. Wang, Journal of Biomedical Materials Research: Part A 86 (2007) 374.
[23] X.Q. Li, Y. Su, C.L. He, H.S. Wang, H. Fong, X.M. Mo, Journal of Biomedical Materials: Part A, doi:10.1002/jbmr, 32286.
[24] F. Hao, Electrospun Polymer, Ceramic, Carbon/Graphite Nanofibers and Their Applications, American Scientific Publishers, California, 2007.
[25] Y.L. Liao, L.F. Zhang, Y. Gao, Z.T. Zhu, H. Fong, Polymer 49 (2008) 5294.
[26] X.Q. Li, Y. Su, X. Zhou, X.M. Mo, Colloids and Surface B: Biointerfaces 69 (2009) 224.
[27] K. Yoon, B.S. Hsiao, B. Chu, Polymer 50 (2009) 2893.
[28] H.T. Zhang, H.L. Nie, S.B. Li, C.B. White, L.M. Zhu, Materials Letters 63 (2009) 1199.